

## The Morphology and Crystallography of Isothermal Martensite in Yttria Stabilized Zirconia

Jae-Hwan Pee,<sup>†</sup> Eui-Seok Choi, and Motozo Hayakawa\*

*Icheon Institute, Korea Institute of Ceramic Engineering and Technology, Seoul 153-801, Korea*

*\*Department of Mechanical Engineering, Tottori University, Koyama Tottori 680-8552, Japan*

(Received October 14, 2005; Accepted November 16, 2005)

### ABSTRACT

A full retention of the tetragonal phase with coarse grains (50~60  $\mu\text{m}$ ) was possible with the specimen  $\text{ZrO}_2$ -1.9 mol%  $\text{Y}_2\text{O}_3$ . In these coarse grains,  $\{101\}_c$  annealing twins were frequently observed, although they do not exist in the usual fine grained specimens. The morphology and growth rate of the isothermally formed individual products are studied at an optical microscopic level. The habit planes of both products are also identified by performing two-surface trace analysis on the grains whose orientations are determined by the Electron Back Scattering Pattern (EBSP) method. The morphologies of isothermal martensite were well-defined thin plates and lenticular types. The growth rate in their longitudinal directions was quite slow and temperature-dependent. A two-surface trace analysis, incorporated with the EBSP method, identified the habit planes near  $\{013\}_c$  in agreement with previous reports obtained from TEM works.

**Key words:** *Isothermal martensitic transformation, Yttria stabilized zirconia, EBSP, Habit plane, Thin plate and lenticular types*

### 1. Introduction

The isothermal and athermal natures of the tetragonal to the monoclinic phase transformation of zirconia and zirconia doped with a small amount of yttria (<1.7 mol%  $\text{Y}_2\text{O}_3$ ) has been well established from recent experiments, which showed the time-temperature dependence of the transformation as well as a burst-type martensitic transformation at subzero temperatures.<sup>1-4)</sup> Even though the isothermal martensitic transformation characteristic may be considered similar to that of the well known isothermal transformation of Y-TZP (Yttria doped Tetragonal Zirconia Polycrystals) except for the higher instability against the stable monoclinic phase, a number of important features are yet unclear. For example, although the temperature dependence of the overall transformation rate has been studied in considerable depth, the knowledge concerning the nucleation and growth mechanisms of an individual product unit and its crystallographic feature has been largely ignored.

For crystallographic study of martensite, single crystals or coarse grains of polycrystals are ideal. Polycrystalline specimens prepared by usual sintering conditions are normally of submicron size and are too small for optical microscopic analysis. However, coarse grains of a single phase can be obtained by annealing at a high temperature, provided

there is a suitable single-phase region for a desired composition at the temperature, as shown in Fig. 1.<sup>5)</sup>

It has been found that the annealing of zirconia doped with 1.9 mol%  $\text{Y}_2\text{O}_3$  at 2273 K for a prolonged period, say 100 h, produces coarse grains as large as 50~60  $\mu\text{m}$  with a suitable stability against the monoclinic phase. Specimens prepared by such methods easily underwent the  $t \rightarrow m$  transformation when heated to around 500 K, or during a subzero cooling to the liquid nitrogen temperature. The occurrence of both isothermal and athermal transformations in the sample of the same chemical composition is very rare. The athermal transformation at a subzero temperature (around 160 K) was first observed in zirconia alloys. For this reason, the transformation characteristics of neither mode have been studied yet; thus it is necessary to investigate the knowledge concerning the microstructure of an individual product unit and crystallographic feature.

In this work, the morphology and growth rate of the isothermally formed individual products are studied at an optical microscopic level. The habit planes of both products are also identified by performing two-surface trace analysis on the grains whose orientations are determined by the Electron Back Scattering Pattern (EBSP) method.

### 2. Experimental Procedure

Powders of the average composition of  $\text{ZrO}_2$ -1.9 mol%  $\text{Y}_2\text{O}_3$  were prepared from pure zirconia and  $\text{ZrO}_2$ -3.0 mol%  $\text{Y}_2\text{O}_3$  powders (TZ-0Y and TZ-3Y, TOSOH, Japan), both having 99.9% purity. They were ball milled with ethanol for 50 h.

<sup>†</sup>Corresponding author : Jae-Hwan Pee  
E-mail : pee@kicet.re.kr  
Tel : +82-2-3282-2435 Fax : +82-2-3282-7750

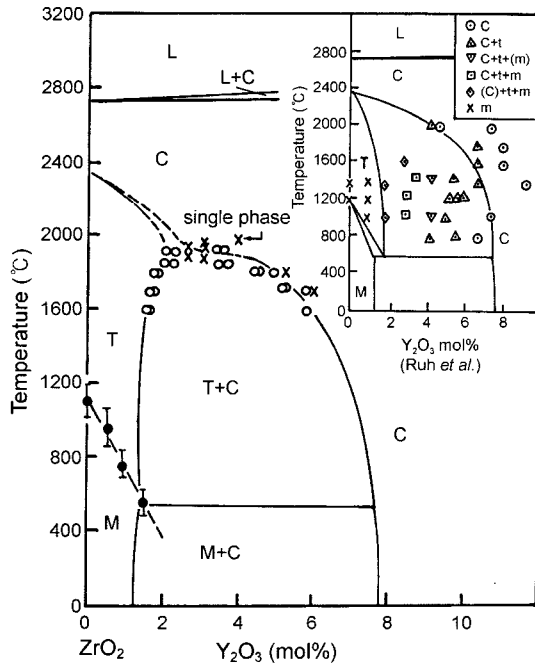


Fig. 1. ZrO<sub>2</sub>-Y<sub>2</sub>O<sub>3</sub> phase diagram. Solid marks; t→m transformation temperature, open marks; maximum and minimum values of Y<sub>2</sub>O<sub>3</sub> determined by EPMA and cross marks; single phase was observed (After Yoshikawa and Suto, 1986).

After being dried, the mixed powders were pressed with a uniaxial pressure of 100 MPa in a steel dies into disks each 19 mm in diameter and 3 mm thick. The disks were sintered at 1723 K for 1 h and then annealed at 2273 K for 100 h in a zirconia furnace (LUVOII-25, Shinagawa Refractory, Japan) to produce a specimen with a large grain size. After the annealing, the specimens were cooled in the furnace to 1273 K then were taken out of the furnace and quenched in water. Although 1.9 mol% Y<sub>2</sub>O<sub>3</sub> is close to the t/t+c phase boundary at 2273 K, the X-ray diffraction study revealed only tetragonal phase, as shown in Fig. 2. The (400)<sub>c</sub> peak of the cubic phase was not observed in coarse grain specimens.

For microscopic observation, the specimen's surface was

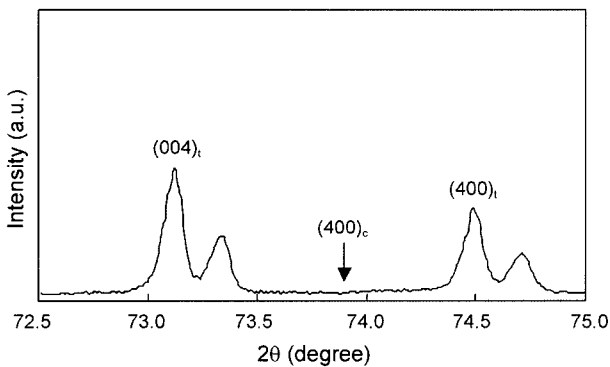


Fig. 2. X-ray diffraction pattern for 1.9Y annealed at 2273 K for 100 h followed by rapid cooling.

polished and thermally etched to reveal the grain boundaries. Chemical etch with 80%HF/20%ethanol was also used when the specimen should not be heated to a high temperature. The surface relieves resulting from the transformation were mostly observed under the Nomarski interference mode but laser microscope and Scanning Electron Microscopy (SEM) were also used. For *in situ* observation of the specimen during transformation, the image was simultaneously recorded on videotape so that the growth rate could be evaluated later on.

A specimen heating stage (LK-600PM, Japan Hitech, Japan) for *in situ* observation was used, which consisted of specimen stage and a heater. A bulk specimen with coarse grains was placed on a silver stage of φ20 mm. The temperature in the vicinity of specimens is measured by a thermocouple (Type K). There was no temperature gradient in the silver plate because of its high thermal conductivity. The specimen stage was covered with a glass-covered window.

The habit planes of the martensite plates were measured by performing standard two-surface trace analysis. Two perpendicular surfaces of a 4×4×10 mm specimen were carefully polished to a 1 μm diamond finish and then heat-treated at 1723 K for 30 min to reveal the grain boundaries and also to remove the residual stress introduced by polishing. The orientations of the grains along an edge were determined by the EBSP/OIM (Orientation Imaging Microscopy) system. EBSPs were produced using a Hitachi S-3000 operated at 20 kV. Because the c/a ratio of the tetragonal phase was small (~1.016), most of the indexing was made in terms of cubic symmetry. Indexing the pattern in terms of tetragonal lattice symmetry was also attempted, which resulted in correct indexing with considerable frequencies.

TEM specimens were prepared from disks cut from a bulk specimen annealed at 2273 K for 100 h. Disks were polished by a diamond slurry (1~9 μm) to ~80 μm thickness. The foils prepared by dimpling and ion beam thinning (CTM-101, COMTEC Inc., Japan) were annealed at 1273 K for 10 min and rapidly cooled by removing them from the furnace to retain a tetragonal phase because the specimen undergoes Ar ion bombarding during the ion thinning process, which increases the temperature of the specimen and promotes the isothermal transformation. The microstructure of a thin foil was examined by a TEM (JEM-2000EX, Jeol, 160 kV, Japan).

### 3. Results and Discussion

Fig. 3 shows a laser micrograph of the parent phase. The average grain size was 25 μm, but a few grains were as large as 50~60 μm. Note that a few grains exhibit bands or domains of slightly different contrast separated by a straight boarder. Such grains were suspected to be twins, as they looked similar to the twins frequently observed in austenitic stainless steel or brass. This can be verified from the lattice orientation and the trace analyses as explained in the following.

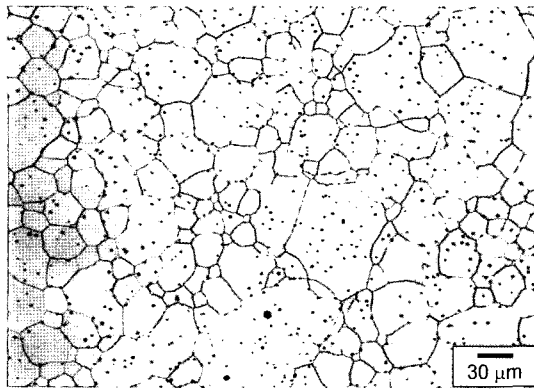


Fig. 3. Laser micrograph of the coarse grained tetragonal phase of 1.9Y after annealing at 2273 K for 100 h and thermal etching at 1723 K for 30 min.

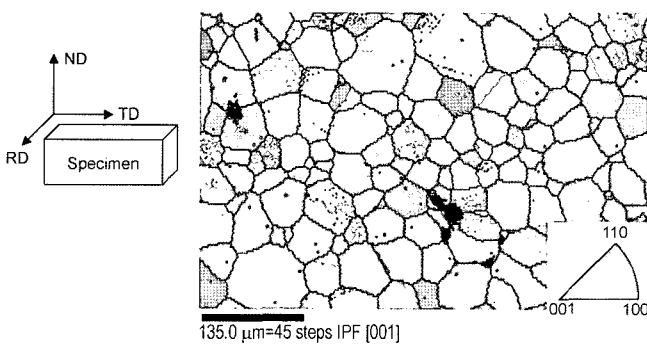


Fig. 4. EBSP orientation map (RD-TD section) of the parent phase. The reference coordinates are referred to as normal direction (ND), rolling direction (RD) and transverse direction (TD).

Fig. 4 shows an example of an EBSP orientation map, where surface normal orientations were plotted based on tetragonal lattice symmetry. The area was scanned by a  $3\mu\text{m}$  step and at each step orientation was measured from the Kikuchi pattern and represented by a colored pixel. As shown in the figure, each grain was mostly covered by pixels of the same color, suggesting that the orientation analyses were mostly successful. Black spots localized near a grain boundary indicate that the orientation could not be determined, probably because of a complex Kikuchi pattern. Sporadic spots of a different color in a grain indicate that the orientation was falsely identified, but a detailed comparison of the orientation with the matrix indicated that only the orientation of the c-axis was mistaken as the a- or b-axis. In fact, the above mentioned twin like bands were observed clearly as different colored regions in EBSP orientation map and they were actually found to be  $\{101\}_t$  twins by the trace analysis.

Twin structures were also found in the TEM works, as shown in Fig. 5(a). From selected area diffraction patterns, it was possible to determine that the area marked (a) ( $[112]_t$  zone axis) represented a tetragonal structure of a different variant from that of the area (b) ( $[211]_t$  zone axis). The annealed 1.9Y crystals are of the single tetragonal phase

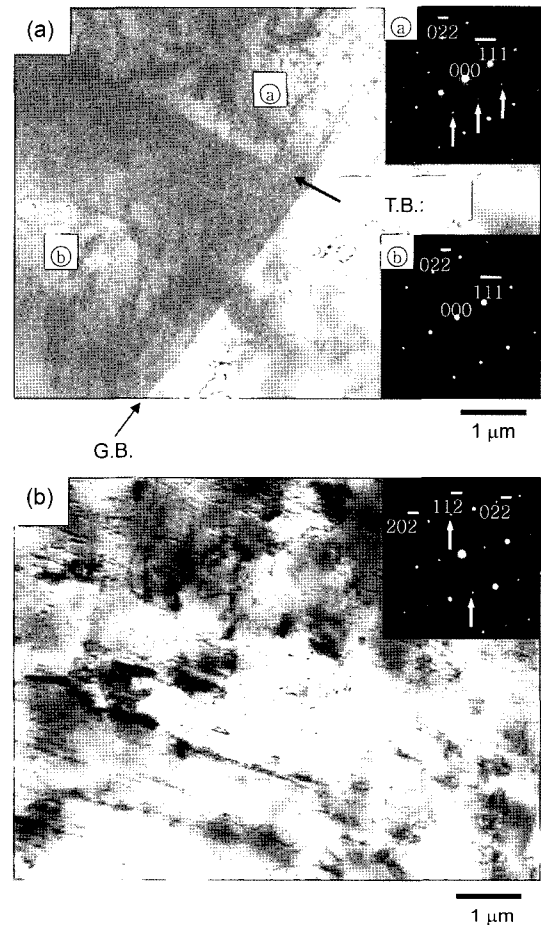


Fig. 5. TEM photographs of 1.9Y showing a tetragonal phase. (a) parent phase containing a twin structure. Diffraction patterns taken from area (a) and area (b), showing  $[112]_t$  and  $[211]_t$  zone, respectively. (T.B.: twin boundary and G.B.: grain boundary) and (b) single tetragonal phase taken from  $[111]_t$  zone, showing  $(112)_t$  reflection.

because the single tetragonal phase taken from the  $[111]_t$  zone gave rise to unique  $(112)_t$  reflection, as shown in Fig. 5(b).

Fig. 6(a)-(c) show a sequence of *in situ* observations of the development of the isothermal martensite at 473 K. When the temperature reached the preset temperature 473 K, there was no nucleated martensite. Plates appeared at 473 K in the 50s and the nucleation appeared to take place mainly at a grain boundary and grew inward the grain. Schubert reported that the thermal expansion anisotropy of  $\dot{Y}$ -TZP can lead to a high residual stresses at grain boundaries making them to be the most likely site for the nucleation of the martensite.<sup>6)</sup> The nucleation of the plates in Fig. 6(a)-(c) and other observations seem to be in agreement with this model. The growth continued until the plate impinged on a grain boundary or other plate at the other end. The plate seemed to thicken mostly after its growth along the longitudinal direction was terminated by one of the events mentioned above (see plate  $A_1$  and  $A_2$  in Fig. 6(b) and (c)).

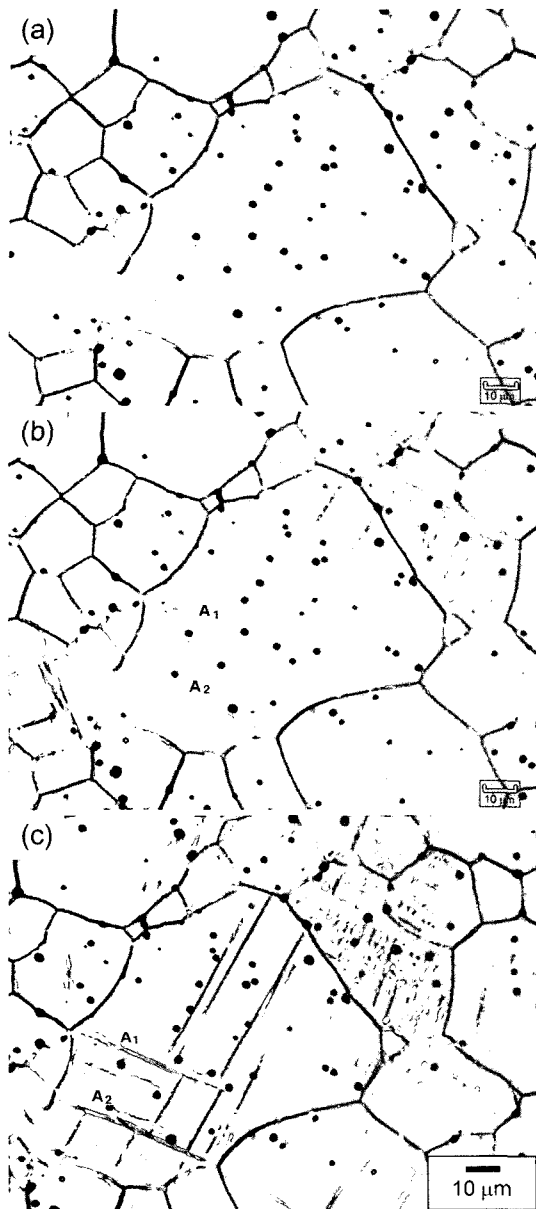


Fig. 6. Laser micrographs showing the sequence of thin plates formation during the isothermal holding at 473 K for (a) 0s, (b) 400s, and (c) 800s.

During the isothermal observation, the growth rate of martensites formed at the beginning appeared to be higher than those formed later. Kurdjumov argued that the first martensite formed might alter the stress state of the retained parent phase in such a way that the formations of new nuclei or their growth become more difficult.<sup>7</sup> However this effect could hardly be important initially because a small quantity of martensite is unlikely to have a significant effect on the retained parent phase. For this reason, the growth rate of plates during isothermal holding was measured only for the plates that appeared during the early stage of transformation.

Fig. 7 shows the growth rate plotted against the holding

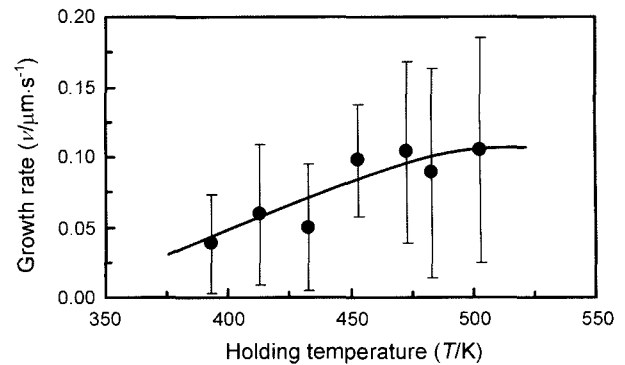


Fig. 7. Growth rate of thin plate martensite in their longitudinal directions as a function of holding temperature.

temperature. Each plotted value is the mean of more than 10 plates in various grains of different size. The vertical bars represent the range of measurements. The large variances in the growth rate at each temperature were mainly due to the greatly varying growth rate from plate to plate depending on the surroundings rather than errors in the measurement. The growth rate in their longitudinal directions was quite slow and temperature-dependent, ranging from 0.03 μm/s at 400 K to 0.10 μm/s at 500 K. In spite of the large variance, the growth rate appears to increase with increasing temperature. However, the growth rate levels off at higher temperatures because the isothermal transformation of this sample proceeds quite fast and the usual heating rate employed for this sample should have intersected the C-curve resulting in transformation (above 510 K).

Fig. 8 shows an SEM micrograph of thin plate formed at 473 K, which was used for a two-surface trace analysis. The surface planes  $S_1$  and  $S_2$  meet perpendicular to each other along the common edge  $E$ . Noted that the trace  $T_1$  on  $S_1$  and trace  $T_2$  on  $S_2$  were continuous at the edge and appear to represent the traces of a thin plate embedded in the body. To confirm that the traces truly represent an embedded thin plate instead of a linear surface martensite, the surface  $S_2$  was polished at about 10 μm and chemically etched. It was possible to observe the trace corresponding to  $T_2$  on the

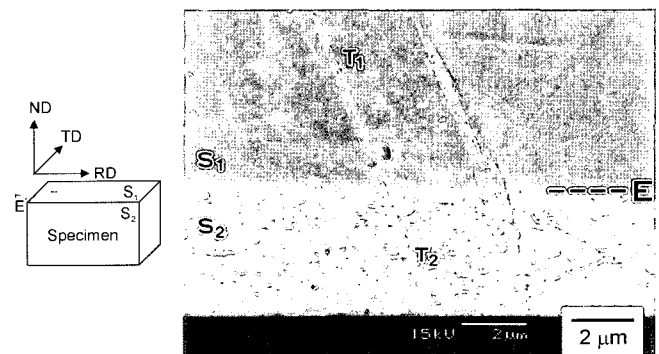


Fig. 8. SEM micrograph of thin plate products whose traces ( $T_1$  and  $T_2$ ) appear on the two perpendicular surface planes  $S_1$  and  $S_2$  with common edge ( $E$ ).

newly exposed  $S_2'$  plane; the fact verified that the traces truly represented an embedded thin plate justifying a two-surface trace analysis.

A standard two-surface trace analysis was applied on the plate illustrated in Fig. 8 and similar ones observed on the grains along edge whose orientation had been identified by the EBSD method. Even though the matrix was tetragonal lattice symmetry, the orientation determination was carried out based on the cubic lattice symmetry because the identification of c-axis from a- and b-axes on the Kikuchi pattern was difficult due to the near unity  $c/a$  ratio. The traces analyses were described in Fig. 9. At first, the sample surfaces are plotted on the Wulff net, and the angle of each trace obtained by each direction is plotted. Then, the habit plane normal is decided by the intersecting point of the trace normal of traces 1 and 2 on the surfaces. These results are summarized in Fig. 10, where the habit plane normals are plotted in an elementary triangle of cubic lattice symmetry.

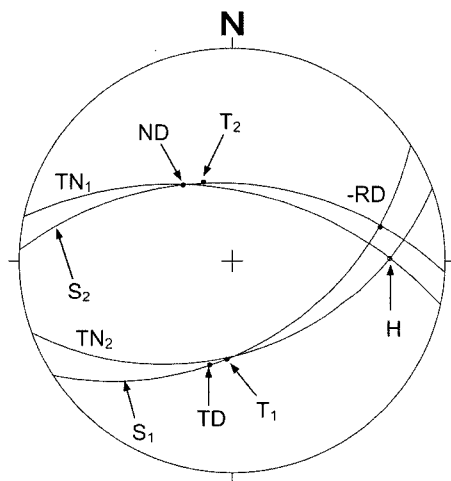


Fig. 9. Stereograph for the traces analysis. The indices without a suffix are those of the cubic basis. (H: Habit plane normal, TN: Trace normal, and S: Surface) (for Fig. 8).

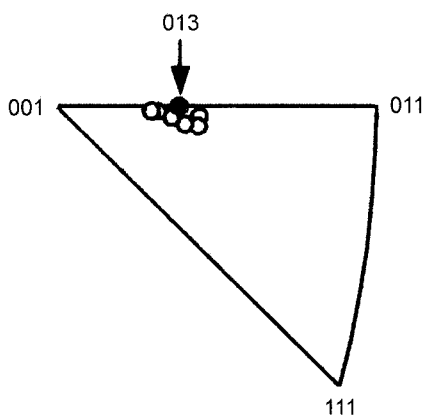


Fig. 10. Habit planes of thin plate products plotted in an elementary triangle of stereo projection based on cubic lattice symmetry.

It can be seen that all six habit plane normals are located near  $\{013\}_c$  within a scatter of several degrees. It is interesting to note that the present habit plane orientation is close to those predicted earlier, i.e.  $(401)_t$  and  $(410)_v$ , and  $(301)_m$  or  $(702)_m$  based on TEM observation and Phenomenological Theory of Martensite Crystallography (PTMC) analysis.<sup>8,9)</sup>

## 4. Conclusions

A full retention of the tetragonal phase with coarse grains was possible with the specimen  $ZrO_2$ -1.9 mol%  $Y_2O_3$ . The average grain size was 25  $\mu m$ , but a few grains were as large as 50~60  $\mu m$ . In these coarse grains,  $\{101\}_t$  annealing twins were frequently observed, although they do not exist in the usual fine grained specimens. The nucleation of isothermal martensite appeared to take place mainly at a grain boundary and grew inward toward the grain. The growth rate in their longitudinal directions was quite slow and temperature-dependent, ranging from 0.03  $\mu m/s$  at 400 K to 0.10  $\mu m/s$  at 500 K. A two-surface trace analysis, incorporated with the EBSD method, identified the habit planes near  $\{013\}_c$  in agreement with previous reports obtained from TEM works.

## REFERENCES

1. M. Hayakawa, K. Nishio, J. Hamakita, and T. Onda, "Isothermal and Athermal Martensitic Transformations in a Zirconia-Yttria Alloy," *Mater. Sci. Eng.*, **273/275** [2] 213-17 (1999).
2. H. Tsubakino and N. Matsuura, "Relationship between Transformation Temperature and Time-Temperature-Transformation Curves of Tetragonal-to-Monoclinic Martensitic Transformation in Zirconia-Yttria System," *J. Am. Ceram. Soc.*, **85** [8] 2102-06 (2002).
3. J. H. Pee, T. Akao, S. Ohtsuka, and M. Hayakawa, "The Kinetics of Isothermal Martensitic Transformation of Zirconia Containing a Small Amount of Yttria," *Mater. Transactions*, **44** [9] 1783-89 (2003).
4. J. H. Pee and M. Hayakawa, "Isothermal and Athermal Type Martensitic Transformations in Yttria Doped Zirconia," *J. Mater. Metallurgy*, **4** [2] 126-31 (2005).
5. N. Yoshikawa and H. Suto, *J. Jpn. Inst. Metals*, **50** 1101-03 (1986).
6. S. Schmauder and H. Schubert, "Significance of Internal Stress for the Martensitic Transformation in Yttria-Stabilized Tetragonal Zirconia Polycrystals During Degradation," *J. Am. Ceram. Soc.*, **69** [7] 534-40 (1986).
7. A. L. Roitburd and G. V. Kurdjumov, "The Nature of Martensitic Transformations," *Mater. Sci. Eng.*, **39** [2] 141-67 (1979).
8. G. K. Bansal and A. H. Heuer, "On a Martensitic Phase Transformation in Zirconia-I. Metallographic Evidence," *Acta Metallurgica*, **20** [11] 1281-89 (1972).
9. M. Hayalawa, N. Kuntani, and M. Oka, "Structural Study on the Tetragonal to Monoclinic Transformation in Arc-Melted  $ZrO_2$ -2 mol% $Y_2O_3$ -I. Experimental Observations," *Acta Metallurgical*, **37** [8] 2223-28 (1989).